Singular Potentials and Anomalous Symmetry Breaking

Author: Andreu Vega Casanovas
Facultat de Física, Universitat de Barcelona, Diagonal 645, 08028 Barcelona, Spain.

Advisor: Tomeu Fiol Núñez

Abstract: This work investigates attractive potentials of the form $1/r^N$ for $N \geq 2$ in Quantum Mechanics. For the inverse square potential ($N = 2$) with sufficiently strong coupling, we examine how classical scale symmetry is broken through the renormalization process, representing the simplest example of a quantum anomaly and touching upon the fundamental question of what symmetries are present in reality. This anomaly is exemplified by the existence of a critical dipole moment required to bind an electron to a polar molecule. In contrast, singular potentials with $N > 2$ exhibit stronger divergences, and we argue why a complete theory cannot be recovered with finitely many parameters, drawing an analogy with nonrenormalizable theories in quantum field theory.
Keywords: Singular potentials, anomalous symmetry breaking, scale invariance, renormalization.
SDGs: This work is related to the sustainable-development goals (ODS) 4 and 9.

I. INTRODUCTION

Quantum mechanics provides a robust framework for describing physical systems governed by various potentials. Standard examples, such as the harmonic oscillator or the Coulomb potential, exhibit well-behaved properties like discrete bound-state spectra and uniquely determined scattering phase shifts. However, a class of potentials known as singular potentials, characterized by a divergence stronger than or equal to $1/r^2$ at the origin, challenges our standard framework and intuition [1]. These exhibit the form

$$V_N(r) = -\tilde{\Gamma}_N/r^N, \quad r \in [0, \infty) \tag{1}$$

and the attractive cases, $\tilde{\Gamma}_N > 0$, are particularly problematic. Indeed, for $N \geq 2$, a naive approach to the resulting dynamics leads to paradoxical results: classically, particles spiral into the centre because no stable orbits exist, even with angular momentum; quantum mechanically, there appears to be no ground state, and bound states seem possible at any negative energy. Furthermore, scattering processes become ambiguous [2, 3].

The inverse square potential ($N = 2$) holds a special, transitional status. While it exhibits pathologies under sufficiently strong attraction ($\tilde{\Gamma}_2 \geq \hbar^2/8m$), it displays a unique connection to classical scale invariance. In three dimensions, it respects the symmetries of the conformal group $\mathrm{O}(1, 2)$ [4]. This marginal behaviour permits renormalization of the theory, breaking scale symmetry and encoding the original coupling into a new parameter that must be determined experimentally. In doing so, it engages with one of the most fundamental questions in physics: what are the true symmetries present in nature?

This anomaly arises in several important systems, including electron binding to polar molecules [5, 6], the interaction of neutral atoms with a charged wire [7], and the capture of matter by a black hole [8].

On the other hand, potentials with $N > 2$ represent truly singular cases. Their stronger divergence at the origin leads to more severe mathematical and physical difficulties, generally rendering them nonrenormalizable in the sense that defining physics requires an infinite number of parameters.

In this work, we study the renormalization of the transitional $N = 2$ potential by introducing an arbitrary cutoff and discuss its implications. Finally, we shed light on the physics underlying the non-renormalizability of more singular potentials and point to a correspondence with renormalization theory in quantum field theory.

II. THE INVERSE SQUARE POTENTIAL

For a central potential, the Hamiltonian commutes with the angular momentum operator, allowing decomposition by angular momentum $\ell \geq 0$. For the case $N = 2$ in Eq. (1), dimensional analysis reveals that the potential and centrifugal barrier contribute equally. Defining $\Gamma_N = 2m\tilde{\Gamma}_N/\hbar^2$, we introduce an effective barrier via $\nu(\nu+1) = \ell(\ell+1) - \Gamma_2$. With $q^2 = 2mE/\hbar^2$, the radial differential equation becomes

$$\left[\frac{d^2}{dr^2} - \frac{\nu(\nu+1)}{r^2} + q^2\right] R_\ell(r) = 0 \ . \tag{2}$$

A. Pathologies and Scale Invariance

We observe that a peculiar property of this scenario already becomes apparent: if we rescale $r \to \beta r$ for $\beta > 0$, then $R_\ell(\beta r)$ remains a solution corresponding to an energy $\beta^2 E$. This is a manifestation of scale invariance, and it implies that the mere existence of a single bound state guarantees the existence of infinitely many bound states with arbitrarily negative energy — and thus, the absence of a ground state. This paradoxical result stems from the lack of an intrinsic energy scale

in the parameters $(\hbar, m, \tilde{\Gamma}_2)$; no combination yields an analogue of the Rydberg energy for the hydrogen atom.

By setting $R_\ell(r) = u_\ell(r)/r$ and $g_\ell = \sqrt{\Gamma_2 - \left(\ell + \frac{1}{2}\right)^2}$, the most general solution takes the form (Appendix A):

$$u_\ell(r) = \sqrt{qr}\left[C_1 J_{ig_\ell}(qr) + C_2 Y_{ig_\ell}(qr)\right] \ . \tag{3}$$

For a repulsive potential, $\Gamma_2 < 0$, g_ℓ is imaginary and there is nothing strange; there are no bound states and, regarding the scattering states, the asymptotic behaviour of the Bessel functions allows us to identify a phase shift which, as expected, does not depend on the energy,

$$\delta_\ell = \frac{\pi}{2}\left(\ell + \frac{1}{2} - ig_\ell\right) \ . \tag{4}$$

For an attractive potential, things start to get complicated when $\Gamma_2 > 1/4$. In this case, some g_ℓ become real, and the solutions oscillate infinitely many times near the origin with $\sqrt{qr}e^{\pm ig_\ell \ln r}$, falling to the centre in the search for a ground state, as displayed in Fig. (1). The following pathologies are found.

- **Bound States:** For any binding energy $E_{bs} = -\hbar^2\mu^2/2m < 0$, a solution can be found in the form $u_\ell(r) \propto \sqrt{\mu r}K_{ig_\ell}(\mu r)$ satisfying $u_\ell(0) = 0$.

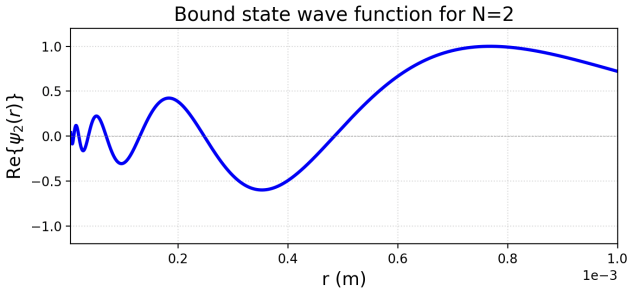

FIG. 1: Bound state wave function for $N = 2$. Note that it oscillates infinitely many times near the origin. If the nodes count the number of lower-energy states, one can always find infinitely many states with lower energy.

- **Scattering States:** For $E > 0$, it is convenient to write the general solution in terms of Hankel functions as

$$u_\ell(r) = \sqrt{r}[C_1 H^{(2)}_{ig_\ell}(qr) + C_2 H^{(1)}_{ig_\ell}(qr)] \ . \tag{5}$$

The condition $u_\ell(0) = 0$ is automatically satisfied. Thus, the ratio C_2/C_1, which determines the reflection amplitude and phase shift, remains undetermined.

B. Regularization and Renormalization

One way to regularize these pathologies is to prevent the fall to the centre by imposing $u_\ell(\varepsilon) = 0$ at a small cutoff $\varepsilon > 0$. This new parameter breaks scale invariance, and the goal will then be to take the limit $\varepsilon \to 0$ and recover some meaningful predictions. We call this strategy renormalization, and we claim that the results obtained in the renormalized theory capture the physics of the original system. For $\mu\varepsilon \ll 1$,

$$K_{ig_\ell}(\mu\varepsilon) \propto \sin\left[g_\ell \log\left(\frac{\mu\varepsilon}{2}\right) - \arg\Gamma(1 + ig_\ell)\right] \ . \tag{6}$$

Bound states arise for $n \geq 1$ upon imposing the aforementioned boundary condition $K_{ig_\ell}(\mu\varepsilon) = 0$,

$$E_{n,\ell} = -\frac{\hbar^2\mu^2_{n,\ell}}{2m} = -\frac{\hbar^2}{2m}\left(\frac{2e^{[\arg\Gamma(1+ig_\ell) - n\pi]/g_\ell}}{\varepsilon}\right)^2 \ . \tag{7}$$

Solutions for $n \leq 0$ are discarded as they violate the assumption that $\mu\varepsilon \ll 1$. As for the scattering states, the cutoff condition, together with the asymptotic behaviour of the solution, yields, for every channel with $g_\ell \in \mathbb{R}$, $e^{2i\delta_\ell} = -iH^{(2)}_{ig_\ell}(q\varepsilon)/H^{(1)}_{ig_\ell}(q\varepsilon)$.

With a bit of algebra and the small-argument expansion of the Hankel functions [9, Sec. 8.4], one can isolate the expression for the scattering phase shift in each channel,

$$\tan\delta_\ell = \frac{\tan\xi + \tanh(\pi g_\ell/2)}{\tan\xi - \tanh(\pi g_\ell/2)} \tag{8}$$

where $\xi = g_\ell \ln(q\varepsilon/2) - \arg\Gamma(1 + ig_\ell)$.

The time has come to eliminate the artificial parameter we introduced—but let's do it carefully! Note that our requirements only fix the product $\mu\varepsilon$, so it is legitimate to ask that as $\varepsilon \to 0$, the constant runs $g_0 \to 0$ in such a way that the ground state energy (for $n = 1$, $\ell = 0$) remains fixed. This implies a scaling

$$g_0(\varepsilon) = -\frac{\pi}{\log(\mu_0\varepsilon/2) + \gamma} \tag{9}$$

where we used that for $g_\ell \ll 1$, then $\arg\Gamma(1 + ig_\ell) = -\gamma g_\ell + O(g_\ell)^2$ with $\gamma \approx 0.577$ is Euler's constant. The price to pay for this procedure is that if $g_0 \to 0$, then all channels with $\ell > 0$ acquire imaginary g_ℓ, removing the pathology—but also eliminating bound states. Similarly, in the $\ell = 0$ channel for $n > 1$, Eq. (7) shows that the bound state energies go to zero. We are thus left with a single bound state.

Returning to the scattering states, all cases lead back to the phase shift given by Eq. (4), except for $n = 1$, $\ell = 0$. In this case, setting $\mu_0 = \mu_{1,0}$, one can revisit Eq. (8) by writing $\xi \approx g_0 \ln(q/\mu_0) - \pi$, obtaining

$$\delta_0(q) = \tan^{-1}\left[\frac{\ln(q/\mu_0) + \pi/2}{\ln(q/\mu_0) - \pi/2}\right] \ . \tag{10}$$

We note that, in order to remove the cutoff, we need to force the parameter of the theory flow towards $\Gamma_2 \to 1/4$. This procedure allows us to extract the phase shift from a single additional parameter, as shown in Fig. (2), which captures the dependence on the original coupling.

The renormalization process, then, has revealed an intrinsic scale in the theory, breaking scale invariance through what is known as a quantum anomaly.

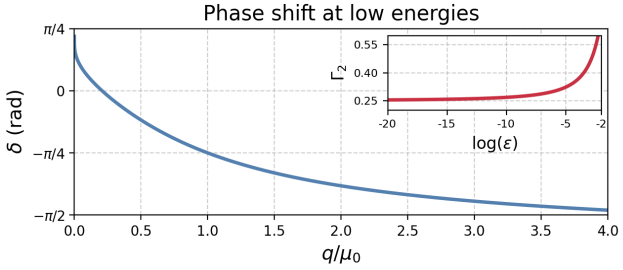

FIG. 2: Phase shift as a function of q/μ_0 for low energy scattering, Eq. (10). The inset shows the logarithmic-like running of the coupling parameter $\Gamma_2 \to 1/4$ with the cutoff parameter $\varepsilon \to 0$ for $\mu_0 = 0.1\ m^{-1}$, Eq. (9).

C. Self-Adjoint Extensions

To make sense of the pathologies in the unrenormalized theory, we have seen how quantum theory acquires an intrinsic scale through renormalization. In doing so, we adjusted the coupling of the theory so that all but one angular channel fall outside the problematic regime. Thus, only the S-channel requires special treatment, where the dependence on the original coupling is absorbed into an unknown parameter. We now turn to a more formal analysis of this procedure.

At the foundations of quantum mechanics lies the requirement that every observable be represented by a self-adjoint operator, ensuring real eigenvalues. However, in the case at hand, we find that the naive theory admits an overabundance of eigenvalues and some of them turn imaginary, a clear symptom of the Hamiltonian's lack of self-adjointness. Indeed, checking Hermiticity via integration by parts reveals a boundary term at $r = 0$ that fails to vanish precisely when $\Gamma_2 > 1/4$.

Fortunately, the requirement of self-adjointness can be relaxed to that of essential self-adjointness, which only requires the existence of a unique self-adjoint extension. To quantify this, von Neumann introduced the deficiency indices (n_+, n_-) [10], which count the eigenvalues of the Hamiltonian of the form $\pm i\eta$, with $\eta > 0$. If $n_+ = n_- = n < \infty$, there exists an n^2-parameter family of self-adjoint extensions; if $n_+ = n_- = 0$, the operator is already self-adjoint; and if $n_+ \neq n_-$, no self-adjoint extension exists. In our case, renormalization required a single parameter to restore consistency, implying $n_+ = n_- = 1$. We will return to this later.

D. Critical Dipole Moment for Electron Binding

The breaking of scale invariance will allow us to explain the existence of an unexpected minimum dipole moment for electron capture by a polar molecule, a phenomenon known as molecular anomaly. Through renormalization, we found that sufficiently strong attractive interactions lead to the existence of a single bound state, and none for weakly attractive and repulsive scenarios. We will see how this threshold determines the critical moment required to bind an electron [5, 6, 11].

The interaction potential between an electron (charge $Q = -e$) and a stationary point dipole $\mathbf{p}$ is given by

$$V(r,\theta) = K_e \frac{(-e)p\cos\theta}{r^2} \tag{11}$$

where θ is the angle relative to the dipole axis. While anisotropic, this potential shares the crucial $1/r^2$ radial dependence and, consequently, the classical scale invariance of the isotropic potential studied previously. Indeed, the coupling can be written in a dimensionless form too,

$$\lambda = \frac{2mK_e}{\hbar^2} ep = \frac{p}{p_0} \tag{12}$$

with $p_0 \approx 1.271$ Debye. By separating variables and introducing the separation constant ζ, we obtain coupled equations for the coordinates r and θ given by

$$\left[\frac{d^2}{dr^2} + \frac{\zeta}{r^2} + q^2\right] u(r) = 0 \tag{13}$$

and

$$\left[-L^2/\hbar^2 + \lambda\cos\theta\right]\Theta(\theta) = \zeta\Theta(\theta). \tag{14}$$

The separation constant is implicitly related to the coupling by means of the eigenvalue equation Eq. (14). As we know, the system undergoes anomalous symmetry breaking at a critical coupling strength of $\zeta \geq \zeta^* = 1/4$. This, at its turn, determines a critical value for the dimensionless dipole coupling $\lambda \geq \lambda^* = 1.279$, which amounts to a critical dipole moment $p^* \approx 1.625$ Debye.

Quantum mechanics predicts that only molecules with a dipole moment $p > p^*$, corresponding to what we identified as the pathological regime, should be capable of binding an electron to form a stable anion. This prediction is remarkably well supported by experimental observations and numerical simulations on a wide range of polar molecules (see Appendix B).

E. Quantum Reflection of Matter Waves

So far, we have discussed the radial inverse square potential generated by a point-like source. We now turn to a related scenario of interest, motivated by recent work [12] in which I have been involved. Here, the setup reduces to one dimension: a particle subject to an attractive $1/z^2$ potential created by a planar surface, where z denotes the distance of the particle from it. The most notable feature of this model is the phenomenon of quantum reflection, in which a quantum particle is scattered off an attractive potential despite the absence of a barrier. Such a configuration can be reproduced

by attaching polar molecules to a planar substrate and reflecting charged particles, as shown in Eq. (11).

Simpleminded boundary conditions trivialize quantum reflection. However, analyzing the effect away from the origin reveals interesting features, motivating the use of tools such as the WKB approximation. Indeed, the wavelike nature of the system prevents a precise identification of a reflection point, making it reasonable to assume that reflection occurs where the WKB approximation breaks down [13]. That is, where the wave function's effective momentum, $p(z) = \sqrt{q^2 - \Gamma_N/z^N}$, oscillates faster than the potential varies. This point corresponds to the maximum of the badlands function

$$B(z) = \hbar^2 \left(\frac{3}{4} \frac{[p'(z)]^2}{p^4(z)} - \frac{1}{2} \frac{p''(z)}{p^3(z)} \right), \tag{15}$$

as noted in [14, p.58]. An analytical expression for the approximate reflection point can be derived, offering a first motivation for implementing such a setup [12]. For $N = 2$, we find (Appendix C):

$$z_0 = \sqrt{|\Gamma_2|}/2q. \tag{16}$$

For a given incident energy, the reflection point seems to consistently occur at the same number of wavelengths. Inserting this into Eq. (5), the reflection probability can be computed by decomposing the potential into linear segments and matching them, solving a Riccati equation.

An apparent scale independence of the reflection probability is found for the inverse square potential—a feature that, at first glance, seems to set it apart from other potentials (see Fig. 3). This suggests that the semiclassical approximation fails to capture the anomaly, providing further motivation for experimental investigation. Whether more refined methods near the origin can reveal the symmetry breaking remains an open question and a direction for future work.

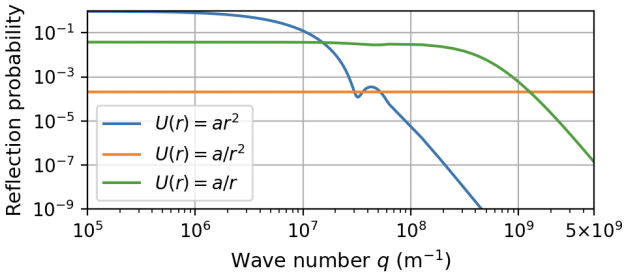

FIG. 3: Naive calculation of the reflection probability as a function of wave number [15] reveals unbroken scale invariance, even in the pathological coupling regime.

III. MORE SINGULAR POTENTIALS ($N > 2$)

We consider now the attractive potential $V(r) = -\tilde{\Gamma}_N/r^N$ with $N > 2$. Dimensional analysis reveals that at short distances, the effect of the potential dominates over the kinetic energy and the centrifugal barrier. This will result in a much stronger fall to the centre [16].

A. Stronger Fall to the centre

With the exception of the case $N = 4$ [1, 17], the derivation of closed-form analytical solutions over the entire domain for the Schrödinger equation with attractive singular potentials is not known. Near the origin, Case suggested a set of algebraic manipulations that allow for a recursive solution to be found [18]. For example, for $N = 3$, ones finds

$$\psi_3(r) = \left(\sqrt{\frac{r}{\Gamma_3}}\right)^{3/2} \left[C_1 e^{2i\sqrt{\Gamma_3/r}} \sum_{n=0}^{\infty} c_n \left(\sqrt{\frac{r}{\Gamma_3}}\right)^n + C_2 e^{-2i\sqrt{\Gamma_3/r}} \sum_{n=0}^{\infty} (-1)^n c_n \left(\sqrt{\frac{r}{\Gamma_3}}\right)^n \right], \tag{17}$$

where

$$c_n = -i\frac{(n+1/2)(n-3/2)}{4n} c_{n-1} - i\frac{q^2\Gamma_3^2}{n} c_{n-5}\,. \tag{18}$$

This is illustrated in Fig. (4). In general, the WKB approximation tells us that near the origin, the solutions will take the form

$$\psi_N \sim r^{N/4} e^{\pm i \frac{2}{N-2}\sqrt{\Gamma_N/r^{N-2}}}\,, \tag{19}$$

in which the phase oscillates infinitely many times as it approaches the origin. While previously these divergences were logarithmic, they now take a power-law form, an indication typically encountered in nonrenormalizable theories.

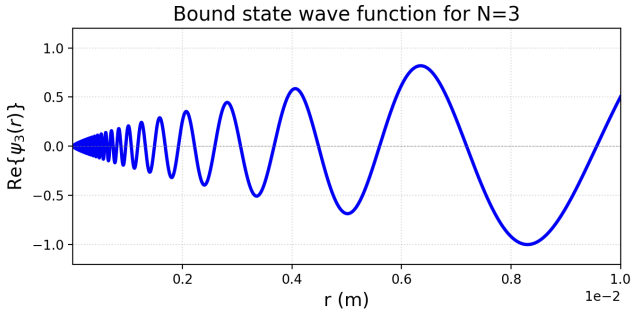

FIG. 4: Bound state wave function for $N = 3$, where sharper oscillations indicate a higher density of bound states and suggest that the previous analysis will be more intricate.

In such cases, repeating the previous strategy becomes more challenging due to the lack of analyticity. However, we note a crucial difference: the dominance of the potential over the centrifugal barrier near the origin causes the different angular momentum channels to decouple. As a result, we cannot rely on the possibility that treating the S-wave channel of the theory will eliminate the pathologies in the other channels $\ell > 0$.

B. Failure of Renormalization

Due to the strong singular behavior at the origin, these potentials yield deficiency indices of $(1, 1)$ for each individual angular channel. However, the decoupling of the channels now necessitates separate renormalization for each, introducing a distinct parameter per case. Consequently, the complete theory would require an infinite set of additional parameters, as the full Hamiltonian exhibits deficiency indices of (∞, ∞) [19, 20]. In other words, if we decompose the Hamiltonian for different angular momenta, $H = \bigoplus_{\ell=0}^{\infty} H_\ell$, so that every H_ℓ acts on a Hilbert space $\mathcal{H}_\ell \subset L^2(\mathbb{R}^3)$, then we will need to provide one parameter for every H_ℓ.

C. Relation to Field Theory

In quantum field theory, nonrenormalizable theories are a common occurrence. In momentum space, the short-distance behavior we have studied translates into high-energy phenomena. As divergences arise at very high energies, they are isolated, and the theory is reformulated as an 'effective theory at low energies'.

In the context of relativistic physics, a canonical example involving a critical coupling constant—beyond which the system develops pathological behavior—is the Coulomb scattering of a Klein–Gordon particle, where the critical coupling is found at $Z_c = 137/2$. In this vein, one can establish a parallel between regular, transitional, and singular potentials and their relativistic analogues. Reference [21] further highlights a correspondence between these systems and, respectively, super-renormalizable, renormalizable, and nonrenormalizable quantum field theories.

IV. CONCLUSIONS

We have seen how renormalization allows us to construct a theory that captures the physics of an originally pathological system. This requires introducing a measurable parameter that absorbs the original coupling. We have shown how the existence of a critical coupling strength helps explain molecular anomalies and motivates experiments on matter-wave reflection off polar substrates. As for singular potentials, the independence of different angular channels requires an infinite number of measurements to renormalize the theory, rendering them nonrenormalizable. The study of quantum anomalies and the transition to singular potentials offers a valuable point of contact with phenomena commonly encountered in quantum field theory.

Acknowledgments

I thank my advisor, Dr. Tomeu Fiol, for his invaluable guidance and advice; Dr. Johannes Fiedler for the insightful conversations and teachings; and my partner, family, and friends for their support and encouragement.

[1] WM Frank, DJ Land, and RM Spector. Singular potentials. *Reviews of Modern Physics*, 43(1):36, 1971.

[2] SA Coon and BR Holstein. Anomalies in quantum mechanics: the $1/r^2$ potential. *American Journal of Physics*, 70(5):513–519, 2002.

[3] Andrew M Essin and David J Griffiths. Quantum mechanics of the $1/x^2$ potential. *American journal of physics*, 74(2):109–117, 2006.

[4] V D'Alfaro, G Furlan, and S Fubini. Conformal invariance in quantum mechanics. *Nuovo Cimento A*, 34(CERN-TH-2115):569–612, 1976.

[5] HE Camblong et. al. Quantum anomaly in molecular physics. *Physical Review Letters*, 87(22):220402, 2001.

[6] C Desfrançois et. al. From $1/r$ to $1/r^2$ potentials: Electron exchange between rydberg atoms and polar molecules. *Physical review letters*, 73(18):2436, 1994.

[7] M Bawin and SA Coon. Neutral atom and a charged wire: From elastic scattering to absorption. *Physical Review A*, 63(3):034701, 2001.

[8] TR Govindarajan et. al. Horizon states for ads black holes. *Nuclear Physics B*, 583(1-2):291–303, 2000.

[9] IS Gradshteyn, IM Ryzhik, and Robert H Romer. Tables of integrals, series, and products, 1988.

[10] D Maksimovič et. al. *Self-adjoint extensions in quantum mechanics*, volume 62. Springer Science, 2012.

[11] Jean-Marc Lévy-Leblond. Electron capture by polar molecules. *Physical Review*, 153(1):1, 1967.

[12] J Fiedler, F Spallek, A Vega, EK Osestad, Q Bouton, and G Dutier. Quantum reflection effects in the diffraction of matter waves. *Submitted to EPL*, 2025.

[13] H Friedrich, G Jacoby, and CG Meister. Quantum reflection by casimir–van der waals potential tails. *Physical Review A*, 65(3):032902, 2002.

[14] H Friedrich. *Theoretical atomic physics*, volume 3. Springer, 2006.

[15] Johannes Fiedler. Private communications, 2025.

[16] LD Landau and EM Lifshitz. *Quantum mechanics: non-relativistic theory*, volume 3. Elsevier, 2013.

[17] RM Spector. *Exact solution of the Schrödinger equation for inverse fourth power potential*, volume 875. University of Rochester, Dptm. of Physics and Astronomy, 1964.

[18] KM Case. Singular potentials. *Physical Review*, 80(5):797, 1950.

[19] H Behncke. Some remarks on singular attractive potentials. *Nuovo Cimento A*, 55(4):780–785, 1968.

[20] H Behncke and H Focke. Deficiency indices of singular Schrödinger operators. *Mathematische Zeitschrift*, 158:87–98, 1978.

[21] A Bastai et. al. On the treatment of singular bethe-salpeter equations. *Nuovo Cimento*, 30:1512–1531, 1963.

Potencials Singulars i Trencament Anòmal de Simetria

Author: Andreu Vega Casanovas
Facultat de Física, Universitat de Barcelona, Diagonal 645, 08028 Barcelona, Spain.

Advisor: Tomeu Fiol Núñez

Resum: Aquest Treball de Fi de Grau investiga el fenomen de caiguda al centre en Mecànica Quàntica arrel de potencials atractius de la forma $1/r^N$ per $N \geq 2$. Pel potencial invers quadràtic ($N = 2$) amb un lligam prou fort, s'examina com la simetria d'escala clàssica és violada mitjançant el procés de renormalització en la teoria quàntica, representant l'exemple més senzill d'anomalia quàntica. Aquesta anomalia és il·lustrada per l'existència d'un moment dipolar crític per tal de lligar un electró a una molècula polar. D'altra banda, potencials singulars amb $N > 2$, els quals presenten divergències més importants, són analitzats, i es raona per què no és possible recuperar una teoria física completa mitjançant la introducció d'un nombre finit de paràmetres, traçant una analogia amb teories no-renormalitzables en teoria quàntica de camps.

Paraules clau: Potencials singulars, trencament anòmal de simetria, invariància d'escala, renormalització.
ODSs: Aquest TFG està relacionat amb els Objectius de Desenvolupament Sostenible (SDGs) 4 i 9.

Objectius de Desenvolupament Sostenible (ODSs o SDGs)

1. Fi de la pobresa		10. Reducció de les desigualtats	
2. Fam zero		11. Ciutats i comunitats sostenibles	
3. Salut i benestar		12. Consum i producció responsables	
4. Educació de qualitat	X	13. Acció climàtica	
5. Igualtat de gènere		14. Vida submarina	
6. Aigua neta i sanejament		15. Vida terrestre	
7. Energia neta i sostenible		16. Pau, justícia i institucions sòlides	
8. Treball digne i creixement econòmic		17. Aliança pels objectius	
9. Indústria, innovació, infraestructures	X		

El contingut d'aquest TFG de la carrera de Física a la Universitat de Barcelona es relaciona amb l'ODS 4, "Educació de qualitat", en ser fruit del treball desenvolupat arrel de la Beca de Col·laboració amb Departaments del Ministeri d'Educació, en el sí Departament de Física Quàntica i Astrofísica de la Universitat de Barcelona sota la supervisió del Prof. Tomeu Fiol. A més, hi ha hagut interessants aportacions fruit de la col·laboració amb un professor de la Universitat de Bergen (UiB).

D'altra banda, donades les aplicacions del contingut del treball en l'explicació d'anomalies presents en sistemes sovintejats en la fabricació de dispositius òptics, també té relació amb l'ODS 9, "Indústria, innovació, infraestructures".

SUPPLEMENTARY MATERIAL

A. Analytic solution for the inverse square potential

I will write down the calculations for $\ell = 0$. The solution for other angular momenta is trivially derived from it.

$$\psi''(r) + q^2\psi(r) + \frac{\Gamma_2}{r^2}\psi(r) = 0 \tag{20}$$

and change $y = 1/r$. By expressing the solution as a descendent power series, we obtain

$$\sum_{n=0}^{\infty} c_n(a-n)(a-n-1)y^{-n-2} + 2\sum_{n=0}^{\infty} c_n(a-n)y^{-n-2} + \Gamma_2\sum_{n=0}^{\infty} c_n y^{-n-2} + q^2\sum_{n=0}^{\infty} c_n y^{-n-4}$$
$$= \sum_{n=0}^{\infty} c_n\Big[(a-n)(a-n+1) + \Gamma_2\Big]y^{-n-2} + q^2\sum_{n=0}^{\infty} c_n y^{-n-4} = 0.$$

For y^{-2}, we get the equation

$$c_0[a(a+1) + \Gamma_2] \to c_0 = 0 \quad \text{or} \quad a = -1/2 \pm \sqrt{1/4 - \Gamma_2}\,.$$

Set $c_0 = 0$ and see that for y^{-3}, we get

$$c_1[(a-1)a + \Gamma_2] = 0 \to c_1 = 0 \quad \text{or} \quad a = 1/2 \pm \sqrt{1/4 - \Gamma_2}\,.$$

We choose the latter and give a solution in terms of c_1. One sees that this choice sets to zero all even coefficients and, for odd coefficients, yields the expression

$$c_{2n+1} = (-1)^n q^{2n} c_1 \prod_{i=0}^{n} \frac{1}{(a-2i-1)(a-2i) + \Gamma_2} = (-1)^n q^{2n}\frac{c_1}{4^n}\prod_{i=0}^{n}\frac{1}{i(i+b)} \tag{21}$$

where we have defined $b = \mp\sqrt{1/4 - \Gamma_2}$. Note now that since the Pochhammer symbols are defined such that $(z)_n = z(z+1)\dots(z+n-1) = \Gamma(n+z)/\Gamma(z)$, we can write

$$c_{2n+1} = (-1)^n q^{2n}\frac{c_1}{4^n}\frac{1}{n!\cdot(b)_{n+1}} \tag{22}$$

and one can write the solution in terms of

$$\psi(y) = c_1 y^{a-1}\sum_{n=0}^{\infty}(-1)^n\frac{1}{n!\cdot(b)_{n+1}}\Big(\frac{q^2}{4y^2}\Big)^n$$

and re-arranging

$$\psi(r) = \frac{c_1}{b}r^{1-a}\sum_{n=0}^{\infty}\frac{(-1)^n}{n!\cdot(b+1)_n}\Big(\frac{r\cdot q}{2}\Big)^{2n} = \frac{c_1\Gamma(b+1)}{b}r^{1/2\mp\sqrt{1/4-\Gamma_2}}\sum_{n=0}^{\infty}\frac{(-1)^n}{n!\cdot\Gamma(n+b+1)}\Big(\frac{r\cdot q}{2}\Big)^{2n}.$$

Now recall that a Bessel function has the form

$$J_\nu(z) = \sum_{n=0}^{\infty}\frac{(-1)^n}{n!\cdot\Gamma(n+\nu+1)}\Big(\frac{z}{2}\Big)^{2n+\nu}.$$

Plugging $C_1 = \frac{c_1\Gamma(b+1)}{b}$ and re-arranging a bit, one sees that we can write $\psi(r) = C_1\sqrt{r}\cdot J_b(q\cdot r)$. For the next step, recall that for non integer ν, the functions $J_\nu(z)$ and $J_{-\nu}(z)$ are linearly independent. Since we have fixed the choice of b, and regarding the form of the Von Neumann functions, a general solution is given by

$$\psi(r) = C_1\sqrt{r}\cdot J_{\sqrt{1/4-\Gamma_2}}(qr) + C_2\sqrt{r}\cdot Y_{\sqrt{1/4-\Gamma_2}}(qr)\ .$$

B. Experimental evidence of molecular anomaly

The renormalization of the inverse square potential has shown that, in sufficiently attractive scenarios, a single bound state exists, while no bound states appear in weakly attractive or repulsive cases. We have interpreted this anomaly as the inability of a polar molecule to bind an electron when the dipole moment is too small and stated that this prediction is supported by both simulations and experiments. The results obtained in [6] are shown below: simulations are represented by solid lines, and experimental data by points.

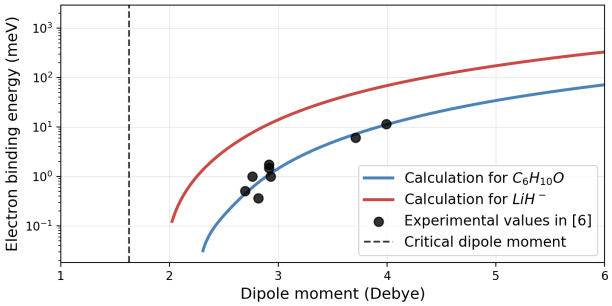

FIG. 5: Simulation and experimental data for electron binding energy as a function of the polar molecule's dipolar moment.

C. Calculation of the approximate reflection point

What follows is based on the supplementary material provided in [12], an article currently under review for publication in EPL, where we outline the derivation of the reflection point. As mentioned, the reflection occurs at the maximum of the badlands function

$$|B(z)| = \left| \hbar^2 \left(\frac{3}{4} \frac{[p'(z)]^2}{p^4(z)} - \frac{1}{2} \frac{p''(z)}{p^3(z)} \right) \right| \ll 1 \,. \tag{23}$$

Let us use the form of a more general potential, $U(z) = \lambda z^N + U_0$, which is singular for $N \leq -2$. It should be noted that we have changed the convention used in the main thesis in order to include more general solutions. A classical returning point can be evaluated by balancing the kinetic and potential energy

$$E = U(z_c) = \lambda z_c^N + U_0 \,. \tag{24}$$

Consequently, the local classical momentum reads

$$p(z) = \sqrt{2m\lambda \left(z_c^N - z^N\right)} \,. \tag{25}$$

We can now plug this into 23, obtaining

$$|B(z)| = \left| \frac{\hbar^2 N m^2 \lambda^2 z^{N-2} \left[\left(\frac{N}{4} + 1 \right) z^N + (N-1) z_c^N \right]}{p(z)^6} \right| \,. \tag{26}$$

In order to maximize this expression, we take the derivative

$$\frac{\mathrm{d}B}{\mathrm{d}z} = \frac{\hbar^2 N z^{N-3}}{8m\lambda (z_c^N - z^N)^4} \left[\frac{(N+4)(N+2)}{4} z^{2N} + \tag{27}$$

$$\frac{(N-1)(5N+8)}{2} z^N z_c^N + (N-1)(N-2) z_c^{2N} \right] \tag{28}$$

and the maximum can be found by writing $t = z^n$ and solving a second-order polynomial, obtaining

$$z^N = z_c^N \frac{-(N-1)(5N+8) \pm N\sqrt{3(N-1)(7N+13)}}{(N+4)(N+2)} \,, \tag{29}$$

where

$$z_c^N = \frac{E - U_0}{\lambda}\,, \tag{30}$$

which can be written as

$$z_0 = \left| \frac{-5N^2 + \left(\sqrt{21N^2 + 18N - 39} - 3\right) N + 8}{N^2 + 6N + 8} \frac{E - U_0}{\lambda} \right|^{1/N} . \tag{31}$$

For $N = -2, -4$, one sees that the denominator diverges. This is, of course, because the quadratic term in Eq. (27) becomes zero. In these cases, going back to Eq. (27), the maximum is found to be in

$$z_0 = \left| \frac{N-2}{\frac{5}{2}N - 4} \right|^{1/N} |z_c| \,. \tag{32}$$

For the case of interest, we note that $N = -2$, $U_0 = 0$ and $\lambda = \tilde{\Gamma}_2$, so that $z_c = \sqrt{|\tilde{\Gamma}_2/E|} = \sqrt{|\Gamma_2|/q^2} = \sqrt{|\Gamma_2|}/q$. Therefore, Eq. (32) reads

$$z_0 = \frac{\sqrt{|\Gamma_2|}}{2q}, \tag{33}$$

as stated in the thesis. This coordinate will be relevant for computing the reflection probability. The strategy will be to approximate the continuous potential by dividing it into linear segments

$$U(z) = U_i \quad , \text{if } z \in [z_i, z_{i+1}] \,, \tag{34}$$

with the discontinuous boundaries located at z_i. The reflection of matter waves at the boundary at $z = z_i$ can be constructed from the elementary reflection and transmission coefficients

$$r_{i,i+1} = \frac{q_{i+1} - q_i}{q_{i+1} + q_i}\,, \quad t = \frac{2q_i}{q_i + q_{i+1}}\,, \tag{35}$$

respectively, via the recursive formula

$$\tilde{r}_{i,i+1} = \frac{r_{i,i+1} + \tilde{r}_{i+1,i+2} \mathrm{e}^{2\mathrm{i}q_{i+1}(z_{i+1} - z_i)}}{1 + r_{i,i+1}\tilde{r}_{i+1,i+2}\mathrm{e}^{2\mathrm{i}q_{i+1}(z_{i+1} - z_i)}}\,. \tag{36}$$

Considering equidistant layering $z_i = \Delta i$ and the wave vector $q_{i+1} = q(z - \Delta)$, the generalised reflection coefficient can be written in continuous variables

$$\tilde{r}(z) = \frac{r(z) + \tilde{r}(z - \Delta)\mathrm{e}^{2\mathrm{i}q(z-\Delta)\Delta}}{1 + r(z)\tilde{r}(z - \Delta)\mathrm{e}^{2\mathrm{i}q(z-\Delta)\Delta}}\,. \tag{37}$$

By taking the continuum limit $\Delta \to 0$ and expanding series, one finds that the reflection coefficient is determined by a Ricatti equation,

$$\tilde{r}'(z) = 2\mathrm{i}q(z)\tilde{r}(z) + \frac{q'(z)}{2q(z)}\left[1 - \tilde{r}^2(z)\right]\,, \tag{38}$$

which must be solved numerically with the appropriate boundary conditions. It is convenient (and realistic) to consider a constant potential beyond the reflection point found in Eq. (33).